Molecular BioSystems

RSC Publishing

PAPER

View Article Online
View Journal | View Issue

Cite this: *Mol. BioSyst.*, 2013, **9**, 412

Structural characterization and biological properties of human gastrokine 1†

Luigi Michele Pavone,[ab] Pompea Del Vecchio,*[c] Paolo Mallardo,[a] Filomena Altieri,[a] Valeria De Pasquale,[a] Silviana Rea,[a] Nicola M. Martucci,[ad] Chiara Stella Di Stadio,[a] Pietro Pucci,[bc] Angela Flagiello,[bc] Mariorosario Masullo,[ad] Paolo Arcari*[ab] and Emilia Rippa[a]

Received 3rd August 2012,
Accepted 5th December 2012

DOI: 10.1039/c2mb25308a

www.rsc.org/molecularbiosystems

Gastrokine-1 (GKN1), a protein expressed in normal gastric tissue, but absent in gastric cancer tissues and derived cell lines, has recently emerged as a potential biomarker for gastric cancer. To better establish the molecular properties of GKN1, the first protocol for the production of mature human GKN1 in the expression system of *Pichia pastoris* was settled. The recombinant protein showed anti-proliferative properties specifically on gastric cancer cell lines thus indicating that it was properly folded. Characterization of structural and biochemical properties of recombinant GKN1 was achieved by limited proteolysis analysis, circular dichroism and fluorescence spectroscopy. The analysis of GKN1 primary structure coupled to proteolytic experiments highlighted that GKN1 was essentially resistant to proteolytic enzymes and showed the presence of at least a disulphide bond between Cys61 and one of the other three Cys (Cys122, Cys145 and Cys159) of the molecule. The secondary structure analysis revealed a prevailing β-structure. Spectroscopic and calorimetric investigations on GKN1 thermal denaturation pointed out its high thermal stability and suggested a more complex than a two-state unfolding process. The resulting protein was endowed with a globular structure characterized by domains showing different stabilities toward chemical and physical denaturants. These results are in agreement with the prediction of GKN1 secondary structure and a three-dimensional structure model. Our findings provide the basis for the development of new pharmaceutical compounds of potential use for gastric cancer therapy.

Introduction

Gastric cancer (GC) is one of the most common solid tumors in the world. High incidence rates are found in Japan, in some regions of East Asia and in some Latin American countries,[1,2] but the rates of mortality and incidence of the disease are very high also in Europe. Despite advances in conventional therapies, the survival rate of patients with GC up to 5 years is poor (<30%), thus GC accounts for the fourth most commonly diagnosed cancer and the second most common cause of cancer-related death worldwide.[3] The etiology of GC is multifactorial including environmental, genetic and infectious factors.[2,4–6] Multiple evidence demonstrated the important role of *Helicobacter pylori* (*H. pylori*) infection in the development of GC.[6–8] Most of the *H. pylori* infected subjects develop acute gastritis, which, if not properly treated, causes chronic disease, and evolves into an ulcer or tumor.[9] In two-thirds of patients in Western countries, GC is diagnosed in an advanced stage, and because this type of tumor is resistant to radiotherapy and chemotherapy, surgery represents the only curative treatment, although often it is only a temporary solution.[10] Therefore, there is an urgent need to clarify the molecular mechanisms underlying the processes of transformation and neoplastic

[a] *Department of Biochemistry and Medical Biotechnology, University of Naples Federico II, Via S. Pansini 5, 80131 Naples, Italy. E-mail: arcari@unina.it; Tel: +39-081-746-3120*
[b] *CEINGE Advanced Biotechnology scarl, Via Gaetano Salvatore 486, 80145 Naples, Italy*
[c] *Department of Chemical Sciences, University of Naples Federico II, Via Cintia, 80126 Naples, Italy. E-mail: pompea.delvecchio@unina.it; Tel: +39-081-674-254*
[d] *Department of DiSIST, University of Naples "Parthenope", Via Medina 40, 80133, Naples, Italy*

† Electronic supplementary information (ESI) available: Supplementary experimental procedure: vector construction and *Pichia pastoris* cell transformation; GKN1 expression and purification; mass spectrometry. Supplementary results: expression and purification of recombinant GKN1; limited proteolysis of GKN1; trypsin digestion of GKN1 in the presence or absence of DTT. Supplementary GKN1 structure prediction: prediction of GKN1 secondary structure; prediction of GKN1 tertiary structure. See: 10.1039/c2mb25308a

progression, to identify new prognostic parameters and to develop more effective therapies for GC.

Recently, the tissue-specific protein gastrokine-1 (GKN1) has emerged as a possible biomarker for GC.[11,12] This protein, expressed in the human stomach of healthy individuals, is absent in gastric adenocarcinoma tissues.[13–15] Some evidence suggests that GKN1 is involved in filling the lumen of the surface layer of epithelial cells to maintain the integrity of the mucosa and to regulate cell proliferation and differentiation.[12,13] As a result of the damage to the gastric mucosa, the presence of GKN1 helps to restore the normal state of the mucosa.[16] In contrast, if the protein is not expressed, the repair process is impaired. It has also been demonstrated that GKN1 expression induces apoptosis in GC cells, indicating the importance of GKN1 in inhibiting the development of GC.[17] Individuals with a lower expression of the protein have an increased risk of developing gastric diseases.[18] The protein, in fact, is downregulated in samples from *H. pylori* infected gastric mucosa and is completely absent in GC.[11,12,14,15] This protein, previously known as 18 kDa antrum mucosal protein (AMP-18), was subsequently called GKN1 by the ''Human Gene Nomenclature Committee'' for its tissue-specific expression and its highly conserved presence in the gastric mucosa of many mammalian species.[12,13] The gene coding for GKN1 (*CA11*) (accession number: BK0017373) is located on chromosome 2.[19] Sequence analysis of the gene showed that the human transcript contains two potential translation start sites (ATG). The first start codon would generate a protein of 199 amino acids whereas the second ATG, located 42 bp downstream, would justify a protein of 185 amino acids. Among the two starting sites, the second appears more possible since it contains a Kozak sequence (GCAGCCAACATG).[20] Comparison of the translated amino acid sequence of human GKN1 with that of other species showed homology only after the second ATG, and its product is predicted to be of 18 kDa. In addition, amino acid sequencing of native GKN1 from pig and N-terminal Edman's degradation of native human GKN1 confirmed that the protein was made of 185 amino acids containing a 20 amino acid extracellular signal peptide localized in the N-terminal region.[13] The protein contains a conserved central structural BRICHOS domain[21] of about 100 amino acids containing two conservative cysteine residues that are possibly involved in disulfide bridges. The putative association of GKN1 with such a domain structure, and with at least three different possible functions, has been proposed, but not conclusively demonstrated. In fact, the BRICHOS domain has been found in proteins with a wide range of functions and disease associations.[22] These include the transmembrane protein BRI2, which is related to familial British and Danish dementia (FBD and FDD); chondromodulin-I (ChM-I), related to chondrosarcoma; CA11, related to stomach cancer; and surfactant protein C (SP-C), related to respiratory distress syndrome (RDS).[21]

Although GKN1 seems to play an important role in gastric mucosa and in the carcinogenic process, a full characterization of its structure and biological activity is still lacking. The purification of the protein from human tissues (normal human antrum mucosa) is very difficult due to the poor availability of human specimens. In order to get more insight into the role of GKN1 in gastric cancer, a recombinant production protocol using the expression system of *Pichia pastoris* (*P. pastoris*) was settled. The recombinant protein was biologically active in the regulation of cellular viability. The physicochemical characterization of the purified recombinant GKN1 was achieved by limited proteolysis, circular dichroism (CD), fluorescence spectroscopy, and microcalorimetry. Bioinformatics tools were used to predict a 3D model of the protein.

Experimental procedures

Microorganisms and culture media

P. pastoris GS115 strain was purchased from Invitrogen, and used as a recombinant protein expression system. Culture media for *P. pastoris* were prepared in Buffered Minimal Glycerol (BMGY) consisting of 100 mM potassium phosphate, pH 6.0, 1.34% yeast nitrogen base (YNB), 0.002% biotin, 1% glycerol, or in Buffered Minimal Methanol (BMMY) consisting of 100 mM potassium phosphate, pH 6.0, 1.34% YNB, 0.002% biotin, 0.5% methanol. Ampicillin was purchased from Sigma, and used at a concentration of 1 mg ml^{-1}.

Cloning and expression of GKN1 in *P. pastoris*

pCDNA3.1 containing the GKN1 cDNA (pCDNA3.1/GKN1)[17] was used to construct a pPIC9K expression vector for the production of recombinant GKN1 in *P. pastoris* according to the procedure reported in the ESI.†[23] The protein concentration was determined according to the Lowry procedure.[24]

Cell culture

Human gastric adenocarcinoma (AGS), human embryonic kidney (HEK293) and human lung epidermoid carcinoma (H1355) cell lines were grown in DMEM-F12 (Dulbecco's modified Eagle medium, Cambrex), DMEM and RPMI (Roswell Park Memorial Institute), respectively, supplemented with 10% heat inactivated fetal bovine serum (FBS), 1% penicillin/streptomycin and 1% L-glutamine at 37 °C in a 5% CO_2 atmosphere. The cells were harvested by treatment with 0.25% trypsin containing 20 mM EDTA, washed with culture medium and re-suspended in complete growth medium for studies of cell proliferation. The cells were maintained in culture for no more than two weeks in order to avoid the protracted passages *in vitro* that alter the metastatic phenotype.

Cell viability assay

Cell proliferation was assessed using a MTT [3-(4,5-dimethylthiazol-2-yl)-2,5-diphenyltetrazolium bromide] assay (Sigma). Re-suspended cells (about 5000 cells per well) were plated in 96-well plates and starved overnight. Cells were then treated with different concentrations of recombinant GKN1 (0.5, 3.0, 5.5, 11.0 and 18.0 μM) for different time intervals (0, 12, 24 and 48 hours or 0, 24, 48 and 120 hours). Subsequently, the MTT solution was added to the wells (0.5 mg ml^{-1} final concentration), and the plates were incubated for additional

4 hours at 37 °C. The reaction was stopped by removing the supernatant followed by the dissolution of the formazan product by the addition of 100 μl of isopropanol. The absorbance at 570 nm was determined using a Bio-Rad ELISA reader. Cell proliferation was expressed as the percentage of formazan formation in the treated samples, compared to the negative control treated only with solvent.

Limited proteolysis

Samples of purified GKN1 (80 μg) were incubated in 20 mM Tris–HCl, pH 7.8, 1 mM $MgCl_2$, 50 mM KCl, 1 mM β-mercaptoethanol with 0.8 μg of trypsin, chymotrypsin or thermolysin at 37 °C in a final volume of 80 μl. At selected times, 20 μl aliquots were withdrawn from the reaction mixture and analysed by SDS-PAGE.[25] The N-terminal amino acid sequence of the products was determined after their transfer on a membrane for microsequencing (Problot) in CAPS using an automatic sequencer (Mod 473 A, Applied Biosystem) connected online to a HPLC apparatus for PTH-amino acid identification.[25]

Western blotting

Proteins were separated by SDS-PAGE, electro-transferred to a PVDF membrane, and incubated for 1 h at room temperature with GKN1 monoclonal antibody, clone 2E5 (Abnova), at 1 : 500 dilution. Anti-mouse secondary antibody conjugated with horseradish peroxidase (HRP) (Santa Crutz, DBA) was used at 1 : 20 000 dilution. The immunoreacted protein bands were visualized using an enhanced chemiluminescence detection reagent (SuperSignal West Pico), exposed to X-ray film, scanned at 1200 dpi resolution and bands were quantified by using Image J software.[26]

Circular dichroism and fluorescence spectroscopy

Sample solutions for spectroscopic measurements were prepared in a 20 mM sodium phosphate buffer at pH 8.5, and the protein concentration was determined by UV absorption reading using a theoretical, sequence-based extinction coefficient of 30 680 M^{-1} cm^{-1} at 280 nm.[27] CD spectra were recorded using a Jasco J-715 spectropolarimeter equipped with a Peltier type temperature control system (Model PTC-348WI). Molar ellipticity per mean residue, $[\theta]$ in deg cm^2 $dmol^{-1}$, was calculated from the equation $[\theta] = [\theta]_{obs}$ mrw/10 lC, where $[\theta]_{obs}$ is the ellipticity measured in degrees, mrw is the mean residue molecular weight of GKN1 (111.3 Da), C is the protein concentration in g ml^{-1} and l is the optical path length of the cell in cm. Molar ellipticity in the near-UV region was calculated per protein molar concentration (m) by using the equation $[\theta] = [\theta]_{obs}100/ml$. CD spectra were recorded by using 0.1 and 0.5 cm path length cells in the far-UV and near-UV region, respectively. For thermal stability studies, spectra were recorded at different temperatures; for denaturant stability investigations, spectra were recorded at 25 °C (constant time 4 s, bandwidth 2 nm, scan rate 20 nm min^{-1}) by varying the GdnHCl or urea concentration. Spectra were signal-averaged over three scans and the baseline was corrected by subtracting the buffer spectrum. Far-UV CD spectra were analyzed for secondary structure estimation by means of the CDSSTR method[28] as implemented in Dichroweb.[29,30]

Thermal unfolding curves were recorded in the far-UV region at 216 nm and 222 nm, and in the near-UV region at 270 nm and 290 nm, from 0 °C to 85 °C, every 0.5 °C with a scan rate of 1 °C min^{-1} at a protein concentration of 0.15 or 1.0 mg ml^{-1} in 0.1 or 0.5 cm cells, respectively. They were analyzed assuming a two-state N ⇆ D unfolding mechanism in order to calculate the denaturation temperature and enthalpy, as previously described.[31] The denaturant-induced unfolding was monitored by following changes in the CD signal at 222 nm of solutions containing an identical concentration of GKN1 in 20 mM sodium phosphate buffer at pH 8.5, which was previously incubated overnight at 25 °C with increasing concentration of GdnHCl or urea. The concentrations of denaturant stock solutions were derived from refractive index measurements.[32] Data were collected using a 0.1 cm path length cell, and ellipticity was averaged over 8 seconds. To estimate the reversibility, the spectra of the unfolded samples of GKN1, upon suitable dilution of denaturant, were recorded at 25 °C. Data were then analyzed in the assumption of a two-state N ⇆ D transition, by means of a linear extrapolation model (LEM).[32] It is assumed that the standard denaturation Gibbs energy change is a linear function of the denaturant concentration [den] according to the equation:

$$\Delta_d G = \Delta_d G_{H_2O} - (m \cdot [\mathrm{den}]) \quad (1)$$

where $\Delta_d G_{H_2O}$ is the value of $\Delta_d G$ in the absence of denaturant and m is a measure of the dependence of $\Delta_d G$ on denaturant concentration. Furthermore, $\Delta_d G_{H_2O} = m \cdot [\mathrm{den}]_{1/2}$, where $[\mathrm{den}]_{1/2}$ is the midpoint of the denaturation process. Denaturation curves were analyzed as already described.[33] Least squares fitting of the data was performed using the software package Origin7.5.

Fluorescence spectra were recorded at 25 °C on a computer assisted Cary Eclipse spectrofluorometer (Varian) at a scan rate of 60 nm min^{-1} using an excitation wavelength of 280 nm; excitation and emission slits were set to 10 nm. The fluorescence spectrum was measured in the range 300–450 nm on samples treated in the absence or in the presence of different denaturant concentrations as reported above.

Differential scanning calorimetry

DSC measurements were performed on a nano-DSC (TA Instruments). The excess molar heat capacity function, $\langle \Delta C_P \rangle$, was obtained after a baseline subtraction, assuming that the baseline is given by the linear temperature dependence of the native-state heat capacity. A buffer–buffer scan was subtracted from the sample scan. The two-state model based van't Hoff enthalpy was calculated by the formula:[34]

$$\Delta_d H(T_d)^{vH} = 4RT_d^2 \langle \Delta C_p(T_d) \rangle / \Delta_d H(T_d) \quad (2)$$

where T_d is the denaturation temperature corresponding to the maximum of the DSC peak, $\langle \Delta C_p(T_d) \rangle$ is the height of the excess heat capacity at T_d, $\Delta_d H^{cal}$ is the total denaturation enthalpy

change calculated by direct integration of the area of the DSC peak and R is the gas constant. A scan rate of 1 °C min and a protein concentration of about 0.4 mg ml^{-1} in 20 mM sodium phosphate buffer, pH 8.5, were chosen for the experiments.

Bioinformatic analysis

Protein secondary structure prediction was done using PSIPRED (Protein Structure Prediction Server, UCL Department of Computer Science, USA). Protein sequences and alignment were obtained from UniProt© 2002–2012 (Universal Protein Resource Consortium, Cambridge, United Kingdom; Geneva, Switzerland; Washington, United States of America). GKN1 3D structural models were computed using I-Tasser Server (Center for Computational Medicine and Bioinformatics, University of Michigan, USA)[35,36] and Swiss Model.[37] Quality assessment of the obtained 3D model was performed using Molprobity server (3D Macromolecular Analysis & Kinemage home page, at the Richardson Laboratory, Department of Biochemistry, Duke University, USA).[38,39] All pdb structures were analyzed and visualized by using the PyMol Molecular Graphics System, Version 1.2r3pre, Schrödinger, LLC.

Results

Expression and purification of recombinant GKN1

The cDNA encoding mature GKN1 (lacking the 20 aa hydrophobic N-terminal region) was cloned into the methanol inducible expression vector pPIC9K, and expressed in *P. pastoris* according to the procedure reported in the ESI† (Fig. S1–S3). The total amount of GKN1 purified from 1 liter of culture medium was around 40 mg.

Biological activity of recombinant GKN1

GKN1 has been reported to affect cell viability,[13] therefore, the ability of the recombinant protein to affect cell proliferation *in vitro* using different cell cultures was evaluated. The results (Fig. 1) showed that GKN1 was endowed with an anti-proliferative effect at a concentration of 0.5 μM after 24 h of treatment of the AGS cell line (Fig. 1A and B). The effect of the protein was dose dependent since the inhibition of cell growth was higher at higher GKN1 concentration. A less marked effect was instead observed using as controls a nongastric cancer cell line (H1355) (Fig. 1C) or a normal cell line (HEK 293) although for the latter higher concentrations of GKN1 were required (Fig. 1D). These results indicated that the recombinant GKN1 was able to exert its function specifically in gastric cancer cells and therefore was appropriate for studying the molecular properties in detail.

Exposed proteolytic sites of recombinant GKN1

The first approach to get an insight into the molecular properties of GKN1 was suggested by the finding that this protein exerted its action in the antrum of the stomach where an extreme environment, characterised by a low pH and the presence of proteases, is found. To this aim, the purified protein was analyzed by limited proteolysis using trypsin, chymotrypsin

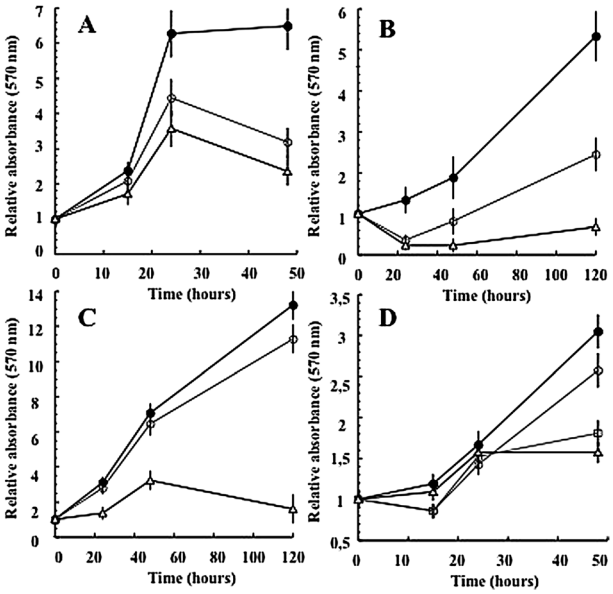

Fig. 1 Effect of GKN1 on cell growth. The effect of GKN1 on cell growth was performed using the MTT procedure after incubation of the cells with GKN1 at different times and concentrations. (A and B) AGS cell growth in the absence (●) or in the presence of 0.5 μM (○) or 3 μM (△) GKN1. (C) H1355 cell growth in the absence (●) or in the presence of 0.5 μM (○) or 3 μM (△) GKN1. (D) HEK 293 cell growth in the absence (●) or in the presence of 5.5 μM (○), 11 μM (△) and 18 μM (□) GKN1, respectively.

and thermolysin. From the SDS-PAGE profile of time-dependent enzymatic digestion, only a few GKN1 fragments were generated (Fig. S4, ESI†), thus indicating that the protein was endowed with an intrinsic compactness, in which proteolytic sites were buried in the solvent. A schematic representation of the proteolytic sites in GKN1 is reported in Fig. 2. In particular, as numbered in mature GKN1, trypsin was able to cleave the protein at the level of Lys89 which was located between Cys61 and the other three cysteines (Cys122, Cys145 and Cys159) whereas chymotrypsin and thermolysin were able to cleave GKN1 mainly at residues located in a region close to the main tryptic site (His64, Tyr101, Phe139 and Lys85 and Phe139, respectively). To test whether the cysteines were involved in a disulfide bond, a trypsin digestion of GKN1 under both reducing and non-reducing conditions was performed. The results obtained (Fig. S5, ESI†) suggested that

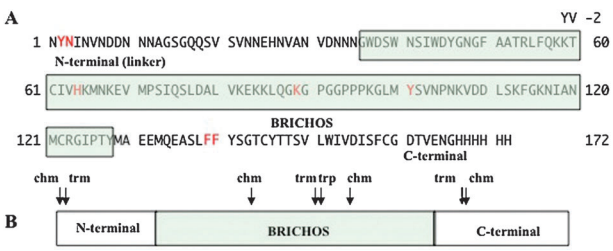

Fig. 2 Schematic representation of GKN1 proteolytic sites. (A) Structural organization and amino acid sequence of recombinant His-tagged GKN1 showing in red the amino acids involved in the proteolytic cleavage. (B) Schematic representation of the proteolytic site position. Chymotrypsin (chm), thermolysin (trm), trypsin (trp).

under non-reducing conditions a disulfide bond between Cys61 and one of the other three cysteines of GKN1 was present.

GKN1 thermal stability

Thermal stability of GKN1 was investigated by both spectroscopic and calorimetric measurements. Fig. 3A shows the far-UV CD spectra of GKN1 in 20 mM phosphate buffer, pH 8.5 recorded at 5 °C (solid line) and 85 °C (dashed line) and at 5 °C after cooling (dotted line). The estimation of the secondary structure content was performed on the spectrum recorded at 5 °C (solid line) by means of the CDSSTR method[28] as implemented in Dichroweb.[29,30] The results indicated that GKN1 possesses a prevailing β-structure in fact, using reference database SP175[40] the calculated secondary structure fractions, with a NRMSD value of 0.021, were: 16% α-helix, 32% β-strands, 12% turns and 40% unordered content. The CD spectrum recorded at 85 °C (dashed line) suggested that the thermal unfolded protein still retained some amount of secondary structure. The far-UV CD spectra of GKN1 recorded from 5 °C to 85 °C, reported in Fig. S6 (ESI†), indicated that small but highly cooperative changes of GKN1 secondary structure occurred at increasing temperature. These changes were very small at 222 nm and more pronounced at 216 nm. Since the CD signals at 222 nm and at 216 nm are characteristic for protein containing α-helix and β-sheet conformation, respectively, to better detect the temperature-induced changes,[41] we recorded thermal denaturation curves at both these wavelengths. The results obtained (Fig. 3B and C) showed a single cooperative inflection point in both cases. The van't Hoff analysis of these thermal unfolding curves yielded a midpoint (T_d) of 81 ±1 °C and the unfolding enthalpy of ΔH^{vH} of 450 ± 27 kJ mol^{-1}. Furthermore, if the heating temperature did not exceed 85 °C, GKN1 thermal denaturation showed to be reversible as revealed by the return of the complete spectrum upon thermal unfolding followed by subsequent cooling to 5 °C (Fig. 3A, dotted line).

Fig. 4A reports the CD spectra of GKN1 in the near-UV region recorded from 5 °C to 85 °C. The spectrum at 5 °C showed a positive band at around 290 nm characteristic of tryptophan residues with a fine structure, and a more intense negative band at around 270 nm characteristic of tyrosine residues with a fine structure. The presence of bands in this spectral region was indicative of a defined tertiary structure of the recombinant

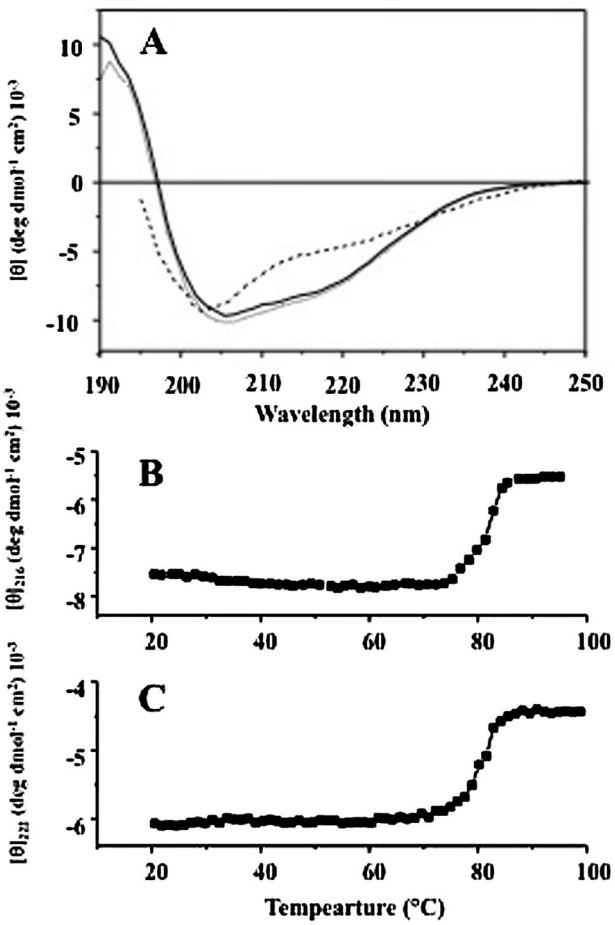

Fig. 3 Far-UV CD spectra of GKN1. (A) Far-UV CD spectra of GKN1 in 20 mM phosphate buffer at pH 8.5, recorded at 5 °C (solid line) or at 85 °C (dashed line); the dotted line represents the spectrum of the latter after cooling at 5 °C. (B and C) Thermal denaturation curve of GKN1 in 20 mM buffer at pH 8.5, recorded by following changes in the CD signal (■) at 216 nm and 222 nm (■), respectively.

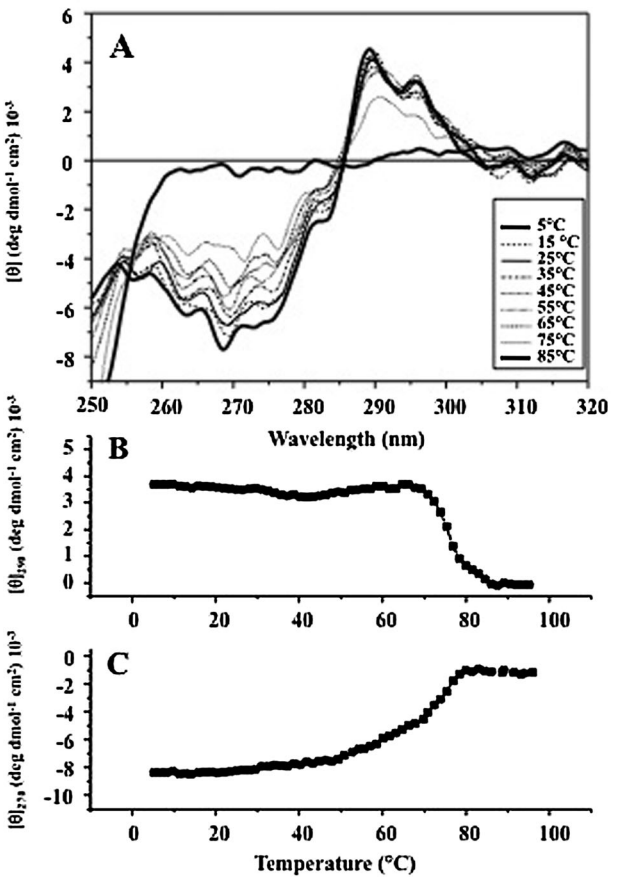

Fig. 4 Near-UV CD spectra of GKN1. (A) Near-UV CD recorded in the temperature interval 5 °C–85 °C. (B and C) Thermal denaturation curves of GKN1 in 20 mM phosphate buffer at pH 8.5, recorded by following changes in the CD signal at 290 nm (■) and 270 nm (■), respectively.

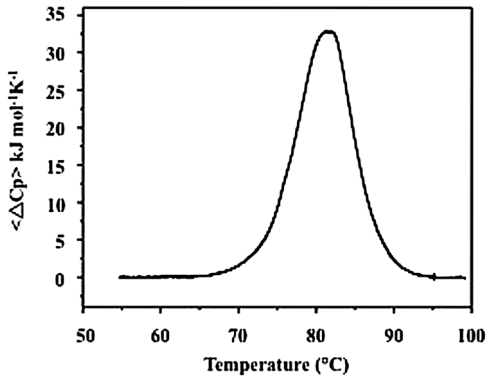

Fig. 5 DSC profile of GKN1 recorded at pH 8.5 in 20 mM phosphate buffer.

GKN1. This fine structure disappeared when the spectrum was recorded at 85 °C. This behaviour clearly indicated that thermal denaturation of GKN1 provoked the complete loss of its tertiary structure. A closer inspection of the denaturation process was carried out by monitoring changes in the CD signal both at 270 nm and at 290 nm as a function of temperature. Both the denaturation curves, reported in Fig. 4B and C, respectively, had a sigmoidal shape with an inflection point at 75 °C, although they clearly showed a different slope especially in the pre-denaturation region. In particular, the change in the CD signal at 270 nm showed a higher slope at increasing temperature, suggesting that, on average, the tyrosine structural proximities are most affected by temperature.

A DSC curve of GKN1, recorded in a 20 mM sodium phosphate buffer at pH 8.5, is reported in Fig. 5. A comparable curve was obtained in a second heating of a sample previously heated up to 80 °C (data not shown). Thus, according to the reheating criterion, the thermal unfolding of GKN1 can be considered as a reversible process. Values of denaturation temperature (T_d) and calorimetric enthalpy change ($\Delta_d H$) were 81.2 ± 0.2 °C and 320 ± 17 kJ mol^{-1}, respectively. The van't Hoff enthalpy change based on a two-state model denaturation process was 450 ± 40 kJ mol^{-1}, in very close agreement with CD results.

GKN1 denaturant-induced unfolding

Denaturant-induced unfolding of GKN1 was investigated by means of CD and fluorescence measurements. Fig. 6A reports the changes in GKN1 molar ellipticity at 222 nm as a function of GdnHCl or urea concentration. The denaturation curves indicated that: (a) GKN1 has a very different resistance towards the denaturing action of GdnHCl and urea; in fact the midpoints corresponding to the denaturant concentration at half-completion of the transition were 1.9 M for GdnHCl and 7.8 M for urea; and (b) a significant content of protein secondary structure was still present in the urea-induced denaturation as indicated by the negative value of the CD signal at 222 nm even at high concentrations of urea. As the denaturant-induced unfolding of GKN1 proved to be a reversible process, a thermodynamic analysis was performed assuming a two state, N ⇆ D model for the unfolding process. The extrapolation to zero

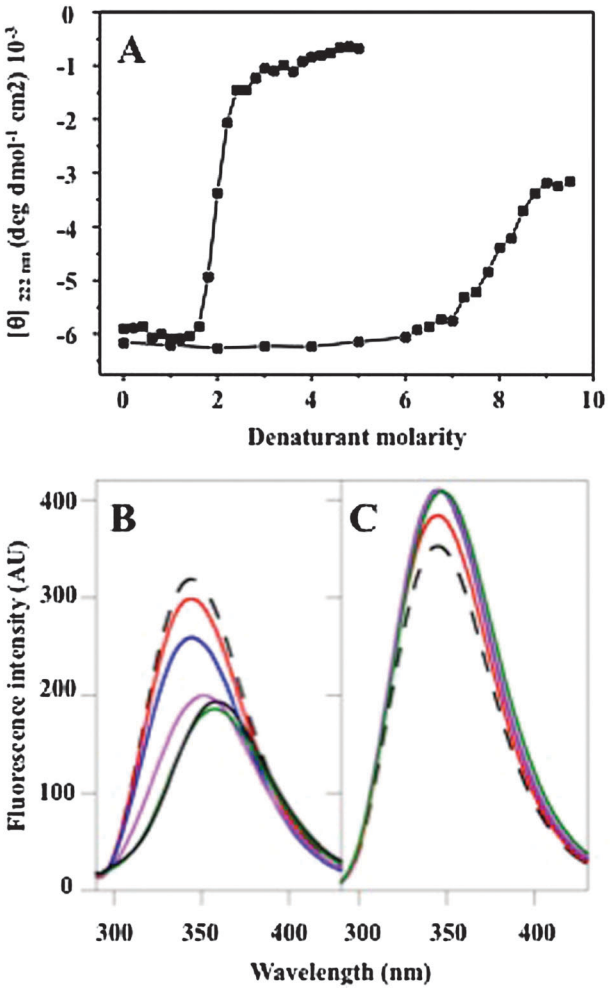

Fig. 6 Urea- and GdnHCl-induced unfolding of GKN1. (A) Change in the CD signal at 222 nm in 20 mM phosphate buffer pH 8.5 and 20 °C at increasing concentration of denaturant. Fluorescence emission spectra of native GKN1 in the absence (dashed line) or in the presence of increasing amounts of GdnHCl (B) and urea (C), respectively.

denaturant concentration resulted in a Gibbs energy difference (ΔG_{H_2O}) of 26.8 ± 2.5 kJ mol^{-1} for GdnHCl and 29.8 ± 3.7 kJ mol^{-1} for urea unfolding, respectively. The corresponding denaturation m values were 14.1 ± 1.3 and 3.7 ± 0.5 kJ mol^{-1} M^{-1} for GdnHCl and urea, respectively.

The fluorescence emission spectrum of GKN1 showed a maximum at 344 nm, upon excitation at 280 nm, that was indicative of a protein with a globular structure[42] in which aromatic residues were rather exposed to the solvent. Even in this case, the spectra recorded upon GdnHCl or urea denaturation denoted a different behaviour between the two denaturants. In particular, at increasing concentration of GdnHCl (Fig. 6B), a significative fluorescence quenching, accompanied by a red shift of wavelength of the maximum, was observed; conversely, at increasing concentration of urea (Fig. 6C), only a small increase in the fluorescence intensity was found. In the case of GdnHCl, the concentration of denaturant for half denaturation derived from either the red-shift in the maximum or the intensity quenching (not shown) was very similar to that

measured in the denaturant-induced unfolding of GKN1 followed by CD. Regarding the effect of urea of the fluorescence spectrum of GKN1, the modest quantum yield increase although did not allow this kind of calculation, still indicated an exceptional resistance of GKN1 to this hydrogen-bond destroyer denaturant.

GKN1 structure prediction

GKN1 homologous sequences including proSPC were selected and aligned using Uniprot server (Fig. S7, ESI†). For each sequence the content of secondary structural elements (H, helix; E, extended; C, coil) was evaluated using PSIPRED server and the predicted structures were compared considering the sequence alignment (Fig. S8, ESI†).

I-Tasser server predicted for recombinant GKN1 five top models on the basis of top ten templates (Table S1 and Fig. S9, ESI†). Swiss Model instead generated a GKN1 3D model using the BRICHOS domain of proSP-C (pdb 2yadA) as a template.[43] The quality of the predicted GKN1 structures was checked using Molprobity server (model 1-3FH and model 1FH, respectively). Comparison of structural parameters of both models (Table S2 and Fig. S10, ESI†) suggested that model 1FH appeared to be more reliable.

Discussion

In this study, the structural and biochemical properties of recombinant human GKN1 lacking the hydrophobic N-terminal peptide, heterologously expressed in the yeast *P. pastoris*, were investigated. The use of this protein expression system was suggested by the fact that the heterologous expression of GKN1 in *E. coli* always gave a product that accumulated into inclusion bodies, even when the expression was carried out at 15 °C (data not shown), and attempts to refold the protein from inclusion bodies were unsuccessful. In contrast, the expression of GKN1 in yeast allowed the production of a soluble form of GKN1 that was purified at high yield. In addition, the capability of recombinant GKN1 to be soluble at relatively high concentration ($\approx$6 mg ml^{-1}) suggested that the protein was correctly folded.[44] This finding was also confirmed by the ability of recombinant GKN1 to exert a higher antiproliferative effect on AGS with respect to H1355 and HEK293 human derived cell lines. The higher sensitivity of AGS cells to GKN1 exposure was likely linked to the role played by GKN1 in maintaining gastric mucosal integrity and to its function as a gastric tumor suppressor. In fact, inactivation of *GKN1* gene in normal gastric cells could play an important role in the development and/or progression of gastric cancer.[45] The data obtained were also in agreement with our previous finding indicating that AGS cells overexpressing GKN1, compared to H1355 cells, showed higher expression of Fas receptor and sensitivity to Fas-ligand induced apoptosis.[17] Therefore, to investigate on the structural features of GKN1, biochemical and spectroscopic properties of the expressed protein were analyzed. To identify exposed regions of GKN1, limited proteolysis experiments were performed showing that the protein was moderately resistant to proteases. Time-course reactions with trypsin, chymotrypsin and thermolysin showed only a partial degradation of the protein with proteolytic cleavages located within the specific region of the protein. Protease resistance was also reported for GKN1 purified from chicken gizzard smooth muscle.[46] However, in the latter case, the protein was cleaved by trypsin only at its N-terminal giving rise to a 18 kDa resistant core protein, in agreement with the evidence that some proteins containing the BRICHOS domain are similarly cleaved.[21] Because GKN1 is highly expressed in human normal stomach mucosal antrum and thus exposed to an harsh environment, its stability against degradation is highly required. Moreover, GKN1 appeared to be further stabilized by the presence of a disulfide bridge occurring between Cys61 and one of the other three cysteine residues (Cys122, Cys145 or Cys159) present in the molecule. However, multiple alignment of several GKN1 homologous proteins (Fig. S7, ESI†), including BRICHOS domain containing proteins such as pulmonary surfactant protein C (PSPC), showed that among all conserved cysteines, only the first two are present in all sequences. In addition, despite the low sequence identities, the prediction of secondary structure of these sequences highlighted from their comparison that the secondary structural elements showed a similar organization (Fig. S8, ESI†). Because in the 3D structure of human proSP-C[43] the first two common cysteines (Cys121 and Cys189) form a disulfide bridge, it is likely that also in GKN1 the corresponding Cys61 and Cys122 might form a bridge. No finding is reported up to now concerning the involvement of GKN1 cysteines in the interaction with other partner proteins, as instead it occurs between the homologous human GKN2 and trefoil factor 1 (TFF1) which were bound through a disulfide bridge.[47,48] However, compared to GKN1, GKN2 contains an additional cysteine residue that could be involved in this interaction.[48]

CD spectroscopy experiments highlighted that GKN1 showed a content of β-structures higher than α-helix. In particular, the far-UV CD spectrum was quite similar to that of β1-proteins showing a positive band at around 190 nm with a negative shoulder at around 220 nm.[49] A prediction of the secondary structure of recombinant GKN1 (33.3% β-sheet and 14.5% α-helix) was consistent with that determined on the basis of CD spectroscopy.

Regarding the thermal stability, our data suggested that the protein was endowed with a considerable high stability for a mesophilic protein, in fact the main cooperative denaturation event occurred above 80 °C as highlighted by calorimetric and far-UV CD thermal denaturation curves. However, the results of near-UV CD thermal denaturation indicated that the protein tertiary structure appeared to be impaired already at 75 °C, thus suggesting that the protein was characterized by the presence of at least two different temperature sensing regions. In fact, the different calorimetric and van't Hoff enthalpy values confirmed that the two-state model did not adequately described the GKN1 thermal denaturation process. Furthermore, the CD melting profiles in the far and near UV suggested that the denaturation process of the protein was more complex than a simple two-state mechanism which leads to a compact

denatured state. The loss of the sharp peaks in the near-UV CD coupled to a much smaller changes in the far-UV CD have been used as a signature to characterize a molten globule state.[50,51]

The GKN1 conformational stability was studied by means of denaturant-induced unfolding measurements. These results indicated that although both urea and GdnHCl affected the GKN1 conformational stability, the latter was four-fold more effective than the urea which likely give rise to a much more compact unfolding state. Urea and GdnHCl have very similar chemical structures and the main difference resides on the fact that the latter is a charged species at neutral pH[52] however, their denaturing effect is different and in particular, GdnHCl mainly affected ion pairs, whereas urea is considered an hydrogen-bonding destroyer.[52] Therefore, the analysis of the concentration of the two denaturants to get an effect indicates that, at least under our experimental conditions, electrostatic interactions play a less important role in the stability of the protein compared to that exerted by hydrogen bonding in GKN1 stabilisation. These results suggest that the high resistance of GKN1 against the denaturing action of urea is possibly due to the role played by hydrogen-forming residues in protein stability. This hypothesis can be supported by the high content of Asn residues (about 13%) present in the protein. In addition, the fluorescence emission spectrum of GKN1 was also in agreement with the predicted GKN1 3D structure in which most of the aromatic residues are rather exposed to the surface.

The structural features determined by CD and fluorescence analyses are in agreement with predictions of secondary structure made for proteins containing the BRICHOS domain.[53] Generally, BRICHOS proteins have four regions: hydrophobic, linker, BRICHOS and C-terminal domains.[22] Residue conservation differs considerably among these regions, however, the BRICHOS region of all components of the protein family showed the highest sequence identity only for two cysteines and one aspartate strictly conserved (D45 in GKN1) thus indicating that this domain should exert a similar function in all the proteins of the family.[22] For instance, the corresponding cysteines in the proSP-C superfamily form an internal disulphide bridge and their strict conservation in the BRICHOS family suggests that the disulphide bridge is also present in all BRICHOS domain members.[54] These findings indicated that these proteins might have well defined tertiary structures.[43] Therefore, 3D GKN1 models were computed using bioinformatic servers and tested for their quality. A plausible model (model 1FH) showed that Cys61 was closer to Cys122 and that the Lys89 was positioned in an almost exposed region in agreement with the proteolytic results. Moreover, the 3D model of GKN1 could be in agreement with the spectroscopic data and suggests the presence in the protein of two distinct domains. The ongoing determination of GKN1 crystallographic structure will clarify these hypotheses.

Conclusions

The data reported on the molecular and functional properties of human GKN1 seem to indicate a more significant propensity for β-sheet structures and this result was coherent with those predicted for the protein families containing the BRICHOS domain. The protein appears to be endowed with an external flexible region susceptible to the action of an ionic chemical denaturant and with a thermal resistant compact region most likely stabilized by strong hydrogen bond. The analysis of the 3D model of the protein suggested that the β-sheet side chains are conserved within BRICHOS domains not only because they are strictly required for formation of the hydrophobic core, but also because they are probably involved in some other functions, such as the possibility of peptide binding as reported for the surfactant protein C. Moreover, the finding that recombinant human gastrokine 1 showed antitumoral properties provides the basis for the development of new pharmaceutical compounds of potential use for gastric cancer therapy.

Abbreviations

AMP-18	18 kDa antrum mucosal protein
BMGY	buffered minimal glycerol
BMMY	buffered minimal methanol
CD	circular dichroism
DSC	differential scanning calorimetry
DMEM-F12	Dulbecco's modified Eagle medium
DTT	dithiothreitol
GC	gastric cancer
FBS	fetal bovine serum
GKN1	gastrokine-1
GdnHCl	guanidinium hydrochloride
HPLC	high performance liquid chromatography
HRP	horseradish peroxidase
MEM	minimum Eagle's Medium
MTT	3-(4,5-dimethylthiazol-2-yl)-2,5-diphenyltetrazolium bromide
NRMSD	normalized root mean square deviation
PTH	phenylthiohydantoin
PVDF	polyvinylidene fluoride
YNB	yeast nitrogen base
YPD	yeast peptone dextrose medium
TFA	trifluoroacetic acid

Acknowledgements

This work was supported by FIRB 2003 (RBLA033WJX_003) to PA and PRIN 2009 to LMP (20097YYPRS_002) and MM (2009P2HZZ7-002). We thank Prof. Francesco Salvatore for critically reading of the manuscript.

References

1 C. Deans, M. S. Yeo, M. Y. Soe, A. Shabbir, T. K. Ti and J. B. So, Cancer of the gastric cardia is rising in incidence in an Asian population and is associated with adverse outcome, *World J. Surg.*, 2011, **35**(3), 617–624.

2 G. J. Krejs, Gastric cancer: epidemiology and risk factors, *Dig. Dis.*, 2010, **28**(4–5), 600–603.
3 M. Bashash, P. Yavari, T. G. Hislop, A. Shah, A. Sadjadi, M. Babaei, A. Brooks-Wilson, R. Malekzadeh and C. Bajdik, Comparison of two diverse populations, British Columbia, Canada, and Ardabil, Iran, indicates several variables associated with gastric and esophageal cancer survival, *J. Gastrointest. Cancer*, 2011, **42**(1), 40–45.
4 D. Forman and V. J. Burley, Gastric cancer: global pattern of the disease and an overview of environmental risk factors, *Best Pract. Res., Clin. Gastroenterol.*, 2006, **20**(4), 633–649.
5 J. Pollock and J. S. Welsh, Clinical cancer genetics: Part I: Gastrointestinal, *Am. J. Clin. Oncol.*, 2011, **34**(3), 332–336.
6 P. Ernst, Review article: the role of inflammation in the pathogenesis of gastric cancer, *Aliment. Pharmacol. Ther.*, 1999, **13**(1), 13–18.
7 M. Cavaleiro-Pinto, B. Peleteiro, N. Lunet and H. Barros, *Helicobacter pylori* infection and gastric cardia cancer: systematic review and meta-analysis, *Cancer, Causes Control, Pap. Symp.*, 2011, **22**(3), 375–387.
8 P. Correa, *Helicobacter pylori* and gastric carcinogenesis, *Am. J. Surg. Pathol.*, 1995, **19**(1), S37–S43.
9 A. Meining, A. Kompisch and M. Stolte, Comparative classification and grading of *Helicobacter pylori* gastritis in patients with gastric cancer and patients with functional dyspepsia, *Scand. J. Gastroenterol.*, 2003, **38**(7), 707–711.
10 D. H. Roukos, Current status and future perspectives in gastric cancer management, *Cancer Treat. Rev.*, 2000, **26**(4), 243–255.
11 K. Shiozaki, S. Nakamori, M. Tsujie, J. Okami, H. Yamamoto, H. Nagano, K. Dono, K. Umeshita, M. Sakon, H. Furukawa, M. Hiratsuka, T. Kasugai, S. Ishiguro and M. Monden, Human stomach-specific gene, CA11, is down-regulated in gastric cancer, *Int. J. Oncol.*, 2001, **19**(4), 701–707.
12 K. A. Oien, F. McGregor, S. Butler, R. K. Ferrier, I. Downie, S. Bryce, S. Burns and W. N. Keith, Gastrokine 1 is abundantly and specifically expressed in superficial gastric epithelium, down-regulated in gastric carcinoma, and shows high evolutionary conservation, *J. Pathol.*, 2004, **203**(3), 789–797.
13 T. E. Martin, C. T. Powell, Z. Wang, S. Bhattacharyya, M. M. Walsh-Reitz, K. Agarwal and F. G. Toback, A novel mitogenic protein that is highly expressed in cells of the gastric antrum mucosa, *Am. J. Physiol.: Gastrointest. Liver Physiol.*, 2003, **285**(2), G332–G343.
14 G. Nardone, E. Rippa, G. Martin, A. Rocco, R. A. Siciliano, A. Fiengo, G. Cacace, A. Malorni, G. Budillon and P. Arcari, Gastrokine 1 expression in patients with and without *Helicobacter pylori* infection, *Dig. Liver Dis.*, 2007, **39**(2), 122–129.
15 G. Nardone, G. Martin, A. Rocco, E. Rippa, G. La Monica, F. Caruso and P. Arcari, Molecular expression of gastrokine 1 in normal mucosa and in *Helicobacter pylori*-related preneoplastic and neoplastic lesions, *Cancer Biol. Ther.*, 2008, **7**(12), 1890–1895.
16 M. M. Walsh-Reitz, E. F. Huang, M. W. Musch, E. B. Chang, T. E. Martin, S. Kartha and F. G. Toback, AMP-18 protects barrier function of colonic epithelial cells: role of tight junction proteins, *Am. J. Physiol.: Gastrointest. Liver Physiol.*, 2005, **289**(1), G163–G171.
17 E. Rippa, G. La Monica, R. Allocca, M. F. Romano, M. De Palma and P. Arcari, Over-expression of gastrokine 1 in gastric cancer cells induces fas-mediated apoptosis, *J. Cell. Physiol.*, 2011, **226**(10), 2571–2578.
18 S. F. Moss, J. W. Lee, E. Sabo, A. K. Rubin, J. Rommel, B. R. Westley, F. E. May, J. Gao, P. A. Meitner, R. Tavares and M. B. Resnick, Decreased expression of gastrokine 1 and the trefoil factor interacting protein TFIZ1/GKN2 in gastric cancer: influence of tumor histology and relationship to prognosis, *Clin. Cancer Res.*, 2008, **14**(13), 4161–4167.
19 Y. Yoshikawa, H. Mukai, F. Hino, K. Asada and I. Kato, Isolation of two novel genes, down-regulated in gastric cancer, *Jpn. J. Cancer Res.*, 2000, **91**(5), 459–463.
20 M. Kozak, An analysis of 5′-noncoding sequences from 699 vertebrate messenger RNAs, *Nucleic Acids Res.*, 1987, **15**(20), 8125–8148.
21 L. Sánchez-Pulido, D. Devos and A. Valencia, BRICHOS: a conserved domain in proteins associated with dementia, respiratory distress and cancer, *Trends Biochem. Sci.*, 2002, **27**(7), 329–332.
22 H. Willander, E. Hermansson, J. Johansson and J. Presto, BRICHOS domain associated with lung fibrosis, dementia and cancer – a chaperone that prevents amyloid fibril formation?, *FEBS J.*, 2011, **278**(20), 3893–3904.
23 J. Sambrook and D. W. Russel, *Molecular Cloning. A Laboratory Manual*, Cold Spring Harbor Laboratory Press, Cold Spring Harbor, NY, 2nd edn, 1989.
24 O. H. Lowry, N. J. Rosebrough, A. L. Farr and R. J. Randall, Protein measurement with the Folin phenol reagent, *J. Biol. Chem.*, 1951, **193**, 265–275.
25 K. Laemmli, Cleavage of Structural Proteins During the Assembly of the Head of Bacteriophage T4, *Nature*, 1970, **227**, 680–685.
26 M. D. Abramoff, P. J. Magalhaes and S. J. Ram, Image Processing with ImageJ, *Biophotonics Int.*, 2004, **11**(7), 36–42.
27 S. C. Gill and P. H. von Hippel, Calculation of protein extinction coefficients from amino acid sequence data, *Anal. Biochem.*, 1989, **182**(2), 319–326.
28 L. A. Compton and W. C. Johnson Jr., Analysis of protein circular dichroism spectra for secondary structure using a simple matrix multiplication, *Anal. Biochem.*, 1986, **155**(1), 155–167.
29 L. Whitmore and B. A. Wallace, DICHROWEB: an online server for protein secondary structure analyses from circular dichroism spectroscopic data, *Nucleic Acids Res.*, 2004, **32**(2), 668–673.
30 N. Sreerama and R. W. Woody, Estimation of protein secondary structure from circular dichroism spectra: comparison of CONTIN, SELCON, and CDSSTR methods with an expanded reference set, *Anal. Biochem.*, 2000, **287**(2), 252–260.
31 P. Del Vecchio, G. Graziano, V. Granata, G. Barone, L. Mandrich, G. Manco and M. Rossi, Temperature- and

denaturant-induced unfolding of two thermophilic esterases, *Biochemistry*, 2002, **41**(4), 1364–1371.

32 C. N. Pace, Determination and analysis of urea and guanidine hydrochloride denaturation curves, *Methods Enzymol.*, 1986, **131**, 266–280.

33 M. M. Santoro and D. W. Bolen, Unfolding free energy changes determined by the linear extrapolation method. 1. Unfolding of phenylmethanesulfonyl alpha-chymotrypsin using different denaturants, *Biochemistry*, 1988, **27**(21), 8063–8068.

34 P. L. Privalov, Stability of proteins: small globular proteins, *Adv. Protein Chem.*, 1979, **33**, 167–241.

35 R. Ambrish, K. Alper and Z. Yang, I-TASSER: a unified platform for automated protein structure and function prediction, *Nat. Protocols*, 2010, **5**(4), 725–738.

36 Z. Yang, I-TASSER server for protein 3D structure prediction, *BMC Bioinf.*, 2008, **9**, 40.

37 K. Arnold, L. Bordoli, J. Kopp and T. Schwede, The SWISS-MODEL workspace: a web-based environment for protein structure homology modelling, *Bioinformatics*, 2006, **22**(2), 195–201.

38 V. B. Chen, W. B. Arendall, J. J. Headd, D. A. Keedy, R. M. Immormino, G. J. Kapral, L. W. Murray, J. S. Richardson and D. C. Richardson, MolProbity: all-atom structure validation for macromolecular crystallography, *Acta Crystallogr., Sect. D: Biol. Crystallogr.*, 2010, **66**, 12–21.

39 I. W. Davis, A. Leaver-Fay, V. B. Chen, J. N. Block, G. J. Kapral, X. Wang, L. W. Murray, W. B. Arendall, J. Snoeyink, J. S. Richardson and D. C. Richardson, MolProbity: all-atom contacts and structure validation for proteins and nucleic acids, *Nucleic Acids Res.*, 2007, **35**(2), W375–W383.

40 J. G. Lees, A. J. Miles, F. Wien and B. A. Wallace, A reference database for circular dichroism spectroscopy covering fold and secondary structure space, *Bioinformatics*, 2006, **22**(16), 1955–1962.

41 *Circular Dichroism and the Conformational Analysis of Biomolecules*, ed. G. D. Fasman, Plenum Publishing Corporation, New York, 1996.

42 V. Rampon, C. Genot, A. Riaublanc, M. Anton, M. A. V. Axelos and D. J. Mcclements, Front-Face Fluorescence Spectroscopy Study of Globular Proteins in Emulsions: Displacement of BSA by a Nonionic Surfactant, *J. Agric. Food Chem.*, 2003, **51**(9), 2482–2489.

43 H. Willander, G. Askarieh, M. Landreh, P. Westermark, K. Nordling, H. Keränen, E. Hermansson, A. Hamvas, L. M. Nogee, T. Bergman, A. Saenz, C. Casals, J. Åqvist, H. Jörnvall, H. Berglund, J. Presto, S. D. Knight and J. Johansson, High-resolution structure of a BRICHOS domain and its implications for anti-amyloid chaperone activity on lung surfactant protein C, *Proc. Natl. Acad. Sci. U. S. A.*, 2012, **109**, 2325–2329.

44 R. Rudolph and H. Lilie, *In vitro* folding of inclusion body proteins, *FASEB J.*, 1996, **10**(1), 49–56.

45 J. H. Yoon, J. H. Song, C. Zhang, M. Jin, Y. H. Kang, S. W. Nam, J. Y. Lee and W. S. Park, Inactivation of the gastrokine 1 gene in gastric adenomas and carcinomas, *J. Pathol.*, 2011, **223**(5), 618–625.

46 K. Hnia, C. Notarnicola, P. de Santa Barbara, G. Hugon, F. Rivier, D. Laoudj-Chenivesse and D. Mornet, Biochemical properties of gastrokine-1 purified from chicken gizzard smooth muscle, *PLoS One*, 2008, **3**(12), e3854.

47 B. R. Westley, S. M. Griffin and F. E. May, Interaction between TFF1, a gastric tumor suppressor trefoil protein, and TFIZ1, a brichos domain-containing protein with homology to SP-C, *Biochemistry*, 2005, **44**(22), 7967–7975.

48 I. Kouznetsova, W. Laubinger, H. Kalbacher, T. Kalinski, F. Meyer, A. Roessner and W. Hoffmann, Biosynthesis of gastrokine-2 in the human gastric mucosa: restricted spatial expression along the antral gland axis and differential interaction with TFF1, TFF2 and mucins, *Cell. Physiol. Biochem.*, 2007, **20**(6), 899–908.

49 N. Sreerama and R. W. Woody, Structural composition of βI- and βII-proteins, *Protein Sci.*, 2003, **12**(2), 384–388.

50 D. A. Dolgikh, R. I. Gilmanshin, E. V. Brazhnikov, V. E. Bychkova, G. V. Semisotnov, S. Yu. Venyaminov and O. B. Ptitsyn, Alpha-lactalbumin: compact state with fluctuating tertiary structure?, *FEBS Lett.*, 1981, **136**(2), 311–315.

51 D. A. Dolgikh, L. V. Abaturov, I. A. Bolotina, E. V. Brazhnikov, V. N. Bushuev, V. E. Bychkova, R. I. Gilmanshin, Yu. O. Lebedev, E. V. Tiktopulo, G. V. Semisotnov and O. B. Ptitsyn, Compact state of a protein molecule with pronounced small-scale mobility: bovine alpha-lactalbumin, *Eur. Biophys. J.*, 1985, **13**(2), 109–121.

52 F. Rashid, S. Sharma and B. Bano, Comparison of Guanidine Hydrochloride (GdnHCl) and Urea Denaturation on Inactivation and Unfolding of Human Placental Cystatin (HPC), *Protein J.*, 2005, **24**(5), 283–292.

53 J. Hedlund, J. Johansson and B. Persson, BRICHOS – a superfamily of multidomain proteins with diverse functions, *BMC Res. Notes*, 2009, **2**, 180.

54 C. Casals, H. Johansson, A. Saenz, M. Gustafsson, C. Alfonso, K. Nordling and J. Johansson, C-terminal, endoplasmic reticulum-lumenal domain of prosurfactant protein C – structural features and membrane interactions, *FEBS J.*, 2008, **275**(3), 536–547.